Recombinant Albumin Mono layers on Latex Particles

4 AUTHORS, INCLUDING:

Kamila Sofińska
Instytut Katalizy i Fizykochemii Powierzchni i…
5 PUBLICATIONS **17** CITATIONS

SEE PROFILE

Zbigniew Adamczyk
Akademickie Centrum Komputerowe CYFRON…
177 PUBLICATIONS **3,709** CITATIONS

SEE PROFILE

Marta Kujda
Polish Academy of Sciences
**13** PUBLICATIONS **80** CITATIONS

SEE PROFILE

Recombinant Albumin Monolayers on Latex Particles

Kamila Sofińska, Zbigniew Adamczyk,* Marta Kujda, and Małgorzata Nattich-Rak

Jerzy Haber Institute of Catalysis and Surface Chemistry, Polish Academy of Sciences, Niezapominajek 8, 30-239 Cracow, Poland

S Supporting Information

ABSTRACT: The adsorption of recombinant human serum albumin (rHSA) on negatively charged polystyrene latex micro-particles was studied at pH 3.5 and the NaCl concentration range of 10^{-3} to 0.15 M. The electrophoretic mobility of latex monotonically increased with the albumin concentration in the suspension. The coverage of adsorbed albumin was quantitatively determined using the depletion method, where the residual protein concentration was determined by electrokinetic measurements and AFM imaging. It was shown that albumin adsorption was irreversible. Its maximum coverage on latex varied between 0.7 mg m^{-2} for 10^{-3} M NaCl to 1.3 mg m^{-2} for 0.15 M NaCl. The latter value matches the maximum coverage previously determined for human serum albumin on mica using the streaming potential method. The increase in the maximum coverage was interpreted in terms of reduced electrostatic repulsion among adsorbed molecules. These facts confirm that albumin adsorption at pH 3.5 is governed by electrostatic interactions and proceeds analogously to colloid particle deposition. The stability of albumin monolayers was measured in additional experiments where changes in the latex electrophoretic mobility and the concentration of free albumin in solutions were monitored over prolonged time periods. Based on these experimental data, a robust procedure of preparing albumin monolayers on latex particles of well-controlled coverage and molecule distribution was proposed.
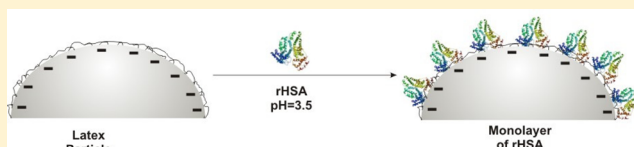
1. INTRODUCTION

Adsorption of human serum albumin (HSA) and the analogous bovine serum albumin at various substrates is an intriguing phenomenon widely studied by a variety of experimental techniques.

These albumins, abundant at a high level, ca. 4−5% in blood plasmas,[1−2] regulate osmotic pressure and transport in the organism of numerous compounds: fatty acids, drugs, metals, and hormones. Hence, HSA is often used for drug delivery and cell therapy products.

Albumins are also used as antiadherent coatings against many bacteria platelets, fibrinogen and IgG in hemodializer membranes, and peacemakers, postoperative infections on orthopedic titanium implants. They are also exploited as blocking agents by preparing immunoglobulin covered latexes used in agglutination immunoassays.[3]

HSA is a single nonglycosylated, α-chain protein consisting of 585 amino acids. Its molecular mass calculated from this amino acid composition is 66439 Da.[2] The crystalline structure of the monomer shown in Table 1 consists of 69% α-helix.[4−6] The BSA molecule exhibits quite an analogous chemical structure and composition as HSA.

Although the molecular shape of albumins is rather irregular, characterized by no symmetry axis (Table 1), one can approximate it by a spheroid having dimensions of 9.5 × 5 × 5 nm[7,8] with the effective cross-section area in the side-on orientation equal to 37 nm^2.

The isoelectric point of fatty acid free HSA is 5.1.[8] The slightly lower value of 4.7 reported in the literature,[2] is characteristic for fatty acid containing samples of HSA. This can also be due to the various buffers used in these studies.[8]

The electric charge distributed heterogeneously over the molecule is mostly due to the glutamic and aspartic acid residues, whereas the positive charge is due to cysteine (Cys), tyrosine (Tyr), lysine (Lys), and arginine (Arg) amino acid residues.[2] The electrokinetic (uncompensated) charge of the HSA molecule is much smaller (in absolute terms) for all pH than the proton charge derived from titration.[4,5,8]

Because of its significance, especially for immunological assays, albumin adsorption on polymeric latex particles has been widely studied with the aim of determining adsorption isotherms for various physicochemical conditions. For example, Norde, Lyklema, and Koutsoukos et al.,[9,10] using the concentration depletion method, determined adsorption isotherms of HSA at polystyrene (PS) latexes. The role of pH (4.0−7.4) and the temperature (5−37 °C) was investigated. No buffers were used in these studies, which makes these measurements particularly valuable.

A similar concentration depletion method (involving the modified Lowry procedure of residual HSA determination) was used for Radomska-Galant and Basińska[11] to determine adsorption isotherms of HSA at PS and polystyrene/polyglicidol (P(S/PGL)) latexes at pH 7.4 (0.2 M phosphate buffer) for bulk HSA concentration up to 500 mg L^{-1}. A considerable adsorption of HSA on the PS latex was observed and practically no adsorption for the P(S/PGL) latex.

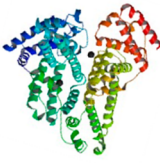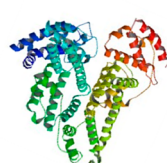Słomkowski et al.[12] determined by the concentration depletion method adsorption isotherm of HSA at polystyrene

Table 1. Physicochemical Properties and the Molecular Shape rHSA (HSA)

Property, Unit	Value		Refs., remarks
	HSA	**rHSA**	
Molecular weight, [Da]	66439	66428	For HSA - from composition[2] For rHSA - from composition (4G03 pdb), calculated in ExPASY Compute pI/Mw tool
Specific density, [g·cm^{-3}]	1.36	1.36	Ref.[2]
Specific volume in crystalline state, [nm^3]	88.3	88.3	Calculated from atomic coordinates[25]
Diffusion coefficient, [cm^2 s^{-1}]	6.1 x 10^{-7}	6.6 - 6.8 x 10^{-7}	For HSA - Ref.[8] (T = 293K) For rHSA measured by DLS for T = 298 K, pH (3.0 - 10.0), 10^{-3} - 0.15 M NaCl
Hydrodynamic diameter, [nm]	7.0	7.2 - 7.4	For HSA - Ref.[8] (T = 293K) For rHSA measured by DLS for T = 298 K, pH (3.5 - 10.0), 10^{-3} - 0.15 M NaCl
Geometrical dimensions, spheroid, [nm]	9.5 x 5 x 5	9.5 x 5 x5	Ref.[8]
Geometrical cross-section area, [nm^2]	37	37	Calculated from geometry
Molecular shape	Monomer of HSA (4EMX from RCSB Protein Data Bank)	Monomer of rHSA (4G03 from RCSB Protein Data Bank)	

(PS) and PSA latexes at pH 7.4 (0.2 M phosphate buffer) for bulk HSA concentration up to 500 mg L^{-1}. The protein coverage determined in this way was correlated with the coverage determined by XPS.

Analogous measurements were performed for BSA using other carrier particles such as colloidal alumina,[7,13] titanium oxide,[14] gold,[15] and so forth.

Despite the complexity of albumin adsorption on carrier particles, two essential regularities were observed in these works. First, it was shown that there appears a fraction of irreversibly bound albumins whose coverage is independent of their initial concentrations in the bulk. This coverage varied between 0.5 and 1.5 mg m^{-2} for lower pH (ionic strength 10^{-3} and 0.15 M) and monotonically decreased with pH. Second, there is also a considerable fraction of albumins whose coverage depends on bulk concentrations and varies between 1 and 2.5 mg m^{-2}. This indicates that this fraction of albumin is reversibly adsorbed and that leads to the appearance of adsorption isotherms. However, quite unexpectedly, in many of the above cited works, little or no desorption of albumins from polymeric carrier particles was observed. This contradiction is probably due to the presence of dimers or higher aggregates in usual albumin samples. These aggregates, exhibiting higher affinity to the polymeric surfaces, can replace, due to Vroman effect, single albumin molecules that were first adsorbed.

Adsorption of albumins on macroscopic (flat) substrates has also been studied both in kinetic and equilibrium aspects. Kinetic measurements of HSA adsorption on glass slides at pH 4−7.4 and I = 0.001−0.1 M were done using the radioisotope techniques by Van Dulm and Norde.[16] The maximum coverage was ca. 1 mg m^{-2} for pH 7.4, I = 0.1 M and ca. 2 mg m^{-2} for pH 4.0, I = 0.1 M.

Elgersma et al.[17] performed measurements of HSA adsorption on various substrates (polystyrene-coated silicon wafers and glass slides) using reflectometry. It was demonstrated that the amount of adsorbed protein (0.8 mg m^{-2}) at pH 4 was independent of its bulk concentration.

Adsorption of HSA at pH 7.4 and ionic strength of 0.15 M on methylated silica was studied by Malmsten[18] using ellipsometry. It was determined that the protein coverage varied between 0.5 and 1 mg m^{-2} depending on the bulk concentration (50 to 1000 mg L^{-1}).

Kurrat et al.[19,20] studied the kinetic of HSA adsorption on hydrated Si and Ti oxides (optical waveguides) using the integrated optics technique (pH 7.4). The maximum coverage of irreversibly bound protein determined in these experiments was 1.7 mg m^{-2}.

Measurements of HSA adsorption on silicon plates were also performed by Ortega−Vinuesa et al.,[21] using ellipsometry methods.

In ref 22, HSA adsorption mechanisms on mica was studied using the in situ streaming-potential method. Adsorption and desorption kinetics of HSA was determined for various ionic strength and pH. It was shown that the amount of irreversibly adsorbed albumin increased with the ionic strength attaining 1.3 mg m^{-2} for I = 0.15 NaCl.

Therefore, the main goal of this paper is to reveal the mechanism of HSA adsorption on colloid latex particles, especially to quantitatively determine the role of ionic strength. The electrophoretic mobility measurements are performed that enable one to monitor the progress of protein adsorption under in situ conditions. In contrast to previous works, the coverage of adsorbed protein is precisely determined via atomic force microscopy (AFM) measurements of the residual albumin concentration without applying the centrifuging step. This enables one to carry out measurements for bulk albumin concentration as low as 0.1 mg L^{-1} that is inaccessible to other methods. In this way, one can unequivocally prove the irreversibility of albumin adsorption for the low concentration range. It should be mentioned that this method has efficiently been used before to determine adsorption mechanism of fibrinogen on latex particles.[23]

Another interesting aspect of our work is the assessment of the validity of the recent electrokinetic model[24] for interpretation of adsorption phenomena on carrier particles previously used to interpret HSA adsorption on mica.[22]

In order to enhance the accuracy of these measurements, the high purity recombinant human serum albumin (hereafter referred to as rHSA) is used. It is characterized by hypoallergenic properties, stability, monomer content, and homogeneity. These properties increase stability of the protein and prevent aggregation. Despite the significance of rHSA, there is little information available in the literature about its physicochemical properties and adsorption process.

2. MATERIALS AND METHODS

2.1. Experimental Section. In our studies, recombinant albumin (rHSA), expressed in *Saccharomyces cerevisiae* and supplied by Sigma (A6608) as aqueous solution was used. The purity of the albumin solutions was checked by dynamic surface tension measurements carried out by the pendant drop shape method. No measurable changes in surface tension of supernatants acquired by ultrafiltration or dialysis of rHSA solutions were observed over a prolonged time period reaching 12 h. The purity of the albumin samples was also determined via SDS-PAGE electrophoresis in Laemmli system[26] using non-reducing sample buffer and 12% polyacrylamide gel. No presence of species having molecular mass below 55 kDa was detected see Figure S1 (Supporting Information).

The bulk concentration of rHSA was determined spectrophotometrically (absorbance measurement at 280 nm), using prepared calibration curve with known concentrations of dissolved standard protein (BSA).

These stock solutions of rHSA of known concentrations (typically 500 mg L^{-1}) were diluted to a desired bulk concentration (usually 0.1−5 mg L^{-1}) prior to each experiment without using any filtration procedure.

Ruby muscovite mica obtained from Continental Trade was used as a substrate for albumin adsorption measurements. Chemical reagents were commercial products of Sigma-Aldrich. Experiments were carried out at the temperature of 298 ± 0.1K.

Polystyrene latex particles synthesized according to the Goodwin method,[27] purified by extensive membrane filtration were used for adsorbing rHSA molecules.

Diffusion coefficients and electrophoretic mobilities of rHSA and latex were measured using dynamic light scattering (DLS) and laser Doppler velocimetry techniques as previously described.

The concentration of rHSA after adsorption on latex was determined using the AFM-based method, shown in Figure 1 and described in detail elsewhere.[28]
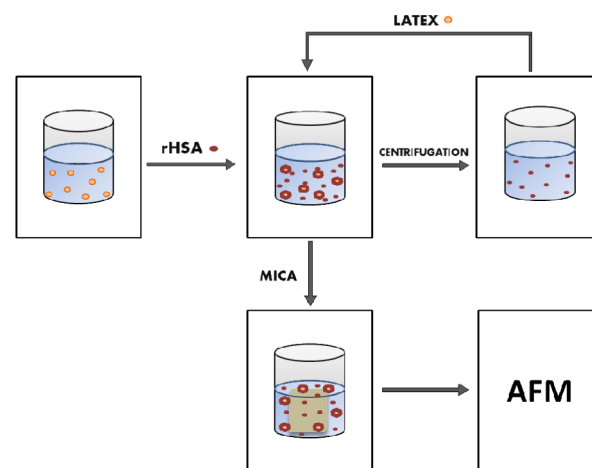
Figure 1. A schematic view of the procedure used for determining rHSA coverage on latex via the microelectrophoresis and AFM methods.

In the first stage, the latex albumin mixture acquired after the adsorption step is allowed to deposit on mica sheets placed in the diffusion cell over a controlled time. Compared to albumin molecules, latex particle deposition was negligible during this time because of its low number concentration and much lower diffusion coefficient. The mica sheets covered by the protein are rinsed and dried. Afterward, the number of albumin molecules was determined over a few equal-sized areas randomly chosen over the mica sheets using AFM imaging. Knowing the averaged number of molecules, the surface concentration and coverage of albumin were calculated in a standard way.

3. RESULTS AND DISCUSSION

3.1. rHSA and Latex Bulk Characteristics. It was determined by DLS that for the NaCl concentration of 10^{-3} to 0.15 M and pH 3.5, the diffusion coefficient of rHSA molecules varied between 6.6−6.8 × 10^{-7} cm^2 s^{-1} (at T = 298 K). Knowing the diffusion coefficient, the hydrodynamic diameter d_a = 7.2−7.4 nm was calculated using the Stokes−Einstein relationship.

The electrophoretic mobility μ_e of rHSA was measured as a function of NaCl concentration at pH 3.5 using the microelectrophoretic method. The experimental data shown in Table 2 and graphically in Figure 2. For NaCl concentration of 10^{-3} M, μ_e = 2.4 × 10^{-8} m^2 (Vs)$^{-1}$ = 2.4 μm cm (Vs)$^{-1}$ (the latter unit is commonly used in the literature). For a NaCl concentration of 10^{-2} M, μ_e = 1.8 μm cm (Vs)$^{-1}$ and for NaCl concentration of 0.15 M, μ_e = 1.1 μm cm (Vs)$^{-1}$. These values correspond to the zeta potential of rHSA molecules equal to 46, 33, and 19 mV, respectively, calculated using the Henry model. It is interesting to mention that the electrophoretic mobilities and zeta potentials of rHSA are markedly lower that the analogous data for the serum HSA (see Table 2).

Table 2. Electrophoretic Mobility μ_e, Zeta Potential ζ (Calculated from the Henry's Model), and Charge Density σ_0 of Latex and rHSA (HSA)

NaCl concentration [M]	latex (L800)			rHSA (HSA)			
	μ_e [μm cm (Vs)$^{-1}$]	ζ [mV]	σ_0 [e nm^{-2}]	μ_e [μm cm (Vs)$^{-1}$]	ζ_{rHSA} [mV]	N_c	σ_0 [e nm^{-2}]
10^{-3}	−6.6	−86	−0.068	2.4 (2.8[a])	46 (53[a])	8.8 (11[a])	0.24 (0.31[a])
10^{-2}	−7.7	−100	−0.25	1.8 (2.1[a])	33 (39[a])	6.6 (8.7[a])	0.18 (0.24[a])
0.15	−4.6	−60	−0.41	1.1 (1.4[a])	19 (23[a])	4.1 (5.7[a])	0.11 (0.15[a])

[a]Previous data from ref 22.
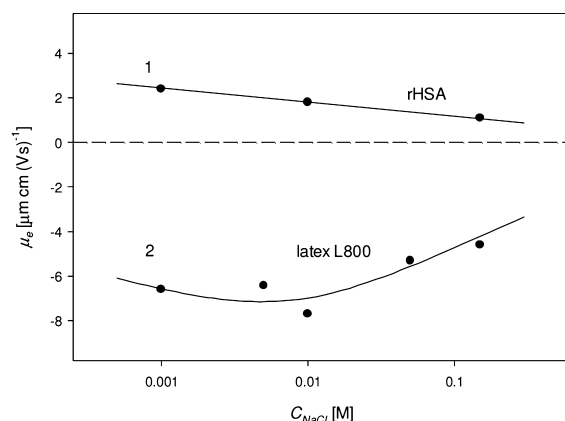
Figure 2. The dependencies of the electrophoretic mobility μ_e [μm cm (Vs)$^{-1}$] of rHSA and latex L800 on the NaCl concentration [M], pH 3.5. The points denote experimental results and the lines represent nonlinear interpolations.

Using the electrophoretic mobility data, one can calculate the electrokinetic charge per albumin molecule Q_c, expressed in Coulombs, from the Lorenz-Stokes relationship[8,29,30]

$$Q_c = 3\pi\eta d_H \mu_e \quad (1)$$

where η is the dynamic viscosity of the solvent (water).

Using Q_c one can calculate the average number of elementary charges per rHSA molecule, denoted by N_c. Values of this parameter obtained for various NaCl concentrations are collected in Table 2.

The hydrodynamic diameter of latex d_l was calculated from its diffusion coefficient measured by DLS. It was 860 ± 15, 850 ± 14, and 810 ± 10 nm for NaCl concentration of 10^{-3}, 10^{-2}, and 0.15 M, respectively.

On the other hand, the electrokinetic charge density of latex particles σ_0 was calculated from the Gouy–Chapman relationship[8,29,30] using zeta potential values collected in Table 2

$$\sigma_0 = \frac{(8\varepsilon k T n_b)^{1/2}}{0.16} \sinh\left(\frac{e\zeta_l}{2kT}\right) \quad (2)$$

where k is the Boltzmann constant, ε is the dielectric permittivity of water, and n_b is the number concentration of the salt (NaCl).

In this way, one obtains from eq 2, $\sigma_0 = -0.068$, -0.25, and -0.41 e nm^{-2} for the NaCl concentration of 10^{-3}, 10^{-2} and 0.15 M, respectively. This corresponds to -0.99, -4.0, and -6.6 μC cm^{-2} for the NaCl concentration of 10^{-3}, 10^{-2} and 0.15 M, respectively.

3.2. Albumin Adsorption on Latex Particles. Primary experimental data concerning albumin adsorption were derived from measurements of the electrophoretic mobility of latex

particles in the protein solutions of controlled concentration. The experimental procedure was as follows:

(i) the reference electrophoretic mobility of bare latex particles was measured;

(ii) rHSA was adsorbed on latex particles by mixing equal volumes of the albumin solution of an appropriate concentration (0.1−5 mg L^{-1}) with the latex suspension of (40−100 mg L^{-1}). The adsorption time was 600 s;

(iii) the electrophoretic mobility of albumin covered latex particles was measured and the corresponding zeta potential was calculated.

The above procedure proved reproducible, enabling a direct evaluation of the electrophoretic mobility and zeta potential variations as a function of the bulk concentration of albumin added to the latex suspension.

It should also be mentioned that the characteristic adsorption time of rHSA on latex particles, estimated in ref 28, was of the order of seconds for the final latex concentration of 100 mg L^{-1}. Therefore, the adsorption time of 600 s ensured that all albumin molecules could adsorb on latex particles.

The primary data obtained in this series of experiments for NaCl concentration of 10^{-2} M are shown in Figure 3 as the dependence of the zeta potential of latex on the initial concentration of the albumin in the suspension (after mixing) denoted by c_H.
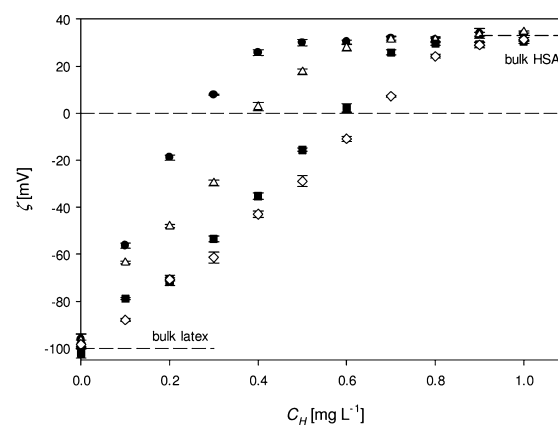
Figure 3. The dependence of the zeta potential of latex ζ [mV] on the initial concentration of rHSA in the suspension c_H expressed in mg L^{-1}. The points denote experimental results obtained for pH 3.5 and various initial latex concentrations: (●) 40 mg L^{-1}, (△) 60 mg L^{-1}, (■) 80 mg L^{-1}, (◇) 100 mg L^{-1}.

As can be seen, the latex zeta potential abruptly increases with the albumin concentration and the slope of this dependence is inversely proportional to the initial latex concentration. This leads to the overcharging effect (inversion of the initial negative zeta potential of latex) for c_H within the range 0.3−0.7 mg L^{-1}. Hence, the results shown in Figure 3

unequivocally demonstrate the sensitivity of the latex adsorption method that can be exploited for detecting albumin concentration at the level of 0.1 mg L^{-1} and below (ca. 10^{-9} M). Additionally, the method is robust, since the time required for measurements can be reduced to seconds and requires minimum amount of latex (ca. 0.5 mg per one measurement). However, in order to make this method quantitative one needs a proper calibration of the experimental data shown in Figure 3 that is achieved using the AFM imaging of single albumin molecules on mica as described later on.

The results in Figure 3 were analyzed by transforming the dependencies obtained for various latex concentration by introducing the nominal coverage of albumin

$$\Gamma_H = \frac{v_s c_H}{S_l} \tag{3}$$

where v_s is the volume of the mixture and S_l is the surface area of latex expressed in m^2, given by $S_l = 6c_l v_s / d_l \rho_l$, where ρ_l is the latex density equal to 1.05×10^3 kg m^{-3}.

Knowing Γ_H, one can also calculate the surface concentration of albumin molecules N_H, from the dependence $N_H = \Gamma_H Av / M_w$, where Av is the Avogadro constant and M_w is the molar mass of albumin.

The experimental data expressed by using eq 3 are plotted in Figure 4.
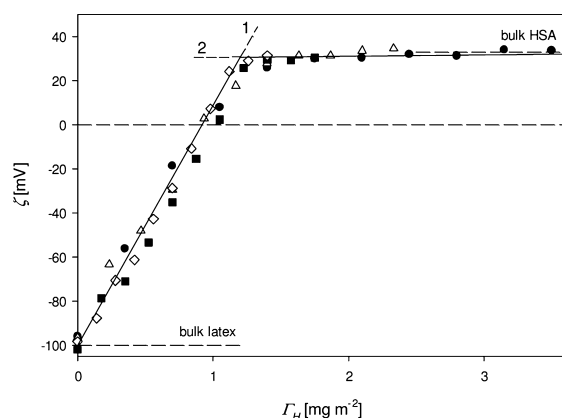
Figure 4. The dependence of the zeta potential of latex ζ [mV] on the nominal coverage of rHSA, Γ_H [mg m^{-2}]. The points denote experimental results obtained for pH 3.5, 10^{-2} M NaCl and various initial latex concentrations 40−100 mg L^{-1}. The intersection of the interpolation lines 1 and 2 shows the extrapolated maximum coverage of rHSA on latex (1.2 mg m^{-2}).

One can observe that the results obtained for various latex concentrations are transformed to a universal relationship characterized by a steep increase in the zeta potential with Γ_H. Afterward, at a critical value of Γ_H, the latex zeta potential attains a plateau value slightly below the bulk zeta potential of albumin (33 mV at this ionic strength). It was also confirmed in a series of additional experiments, that there were no changes in the electrophoretic mobility (zeta potential) of latex over time periods up to 500 h. This suggests that albumin adsorption was irreversible because the zeta potential of latex was only dependent on the albumin coverage rather than on its bulk concentration. Moreover, by exploiting the data shown in Figure 4, one can estimate the maximum coverage of albumin from the intersection of the lines fitting the results for lower coverage and the horizontal straight line (see Figure 4). In this

way one obtains 1.2 mg m^{-2} as the plausible value of the maximum coverage of rHSA on latex particles.

Analogous measurements as these shown in Figure 4 were performed for other ionic strengths.

It should be mentioned that the results shown in Figure 4 are similar to previously obtained by Serra et al.[31] for the polyclonal rabbit immunoglobulin (IgG) who observed that for pH 5 and I = 5×10^{-2} M, the electrophoretic mobility of the polystyrene latex abruptly increases with the IgG coverage and attains positive values for the coverage higher than 2 mg m^{-2}. Similar data were also reported in ref 23 for human serum fibrinogen adsorption on the same latex L800 particles used in our work.

As previously done,[28] the experimental dependencies shown in Figure 5 were interpreted in terms of the mean-field Gouy−Chapman (GC) model, where the protein molecules are assumed to adsorb underneath the shear plane and the three-dimensional (3D) model where it is assumed that the molecules adsorb as discrete particles on the latex surface, sticking-out from the shear plane.[24,32,33]

Accordingly, in the case of the GC model it is postulated that the net charge density is given by[22,30,32]

$$\sigma = \sigma_0 + eN_c \left(\frac{Av}{M_w} \right) \Gamma_H \tag{4}$$

where σ_0 is the surface charge density of bare latex particles given in Table 2.

Knowing the charge density one can calculate the zeta potential of latex particles covered by rHSA using the relationship[23,32]

$$\zeta = \pm \frac{2kT}{e} \ln \frac{|\bar{\sigma}| + (\bar{\sigma} + 4)^{1/2}}{2} \tag{5}$$

where the plus and minus sign corresponds to the positive and negative sign of σ, $\bar{\sigma} = \sigma / (2\varepsilon kT n_b)^{1/2}$ is the dimensionless electrokinetic charge density and n_b is the electrolyte concentration.

As can be seen in Figure 5, the theoretical results derived from the GC model (depicted by the dashed−dotted line) reasonably agree with our experimental data only for the NaCl concentration of 10^{-3} M. For higher NaCl concentrations of 10^{-2} and 0.15 M, the GC model is inadequate since it considerably underestimates the experimental data.

This indicates that for higher ionic strength, a significant part of adsorbed albumin molecules is located above the shear plane that enhances the rate of zeta potential variations. Hence, in this case, the 3D electrokinetic model should be more appropriate. According to this model, the following expression for the zeta potential of interfaces covered by protein molecules can be formulated[24,33]
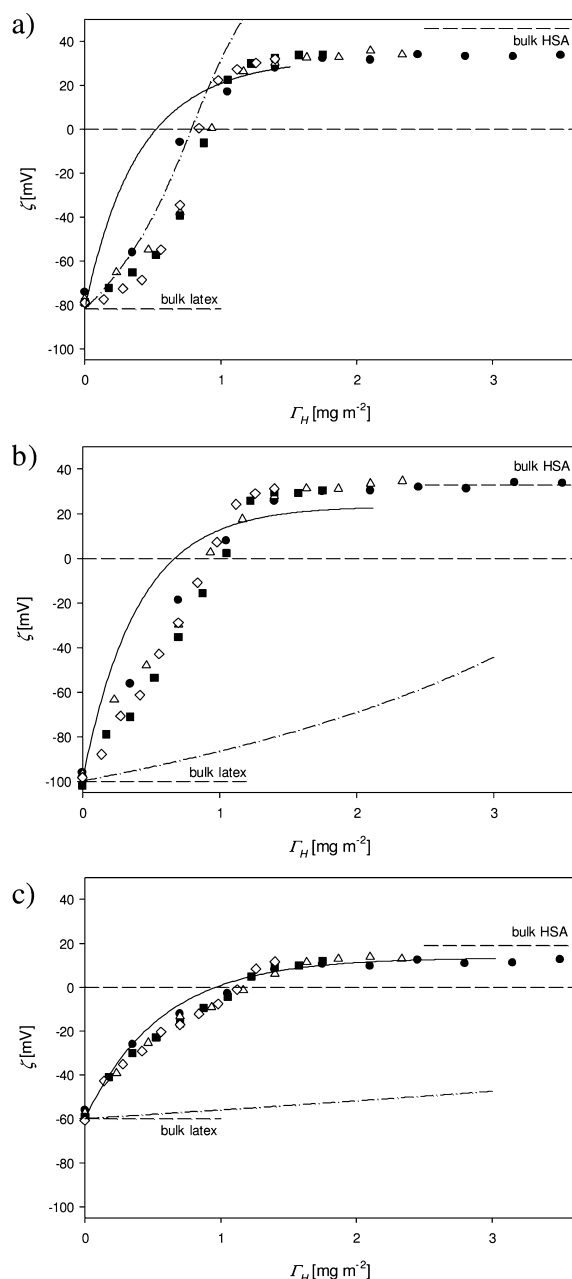
$$\zeta(\Theta) = F_i(\Theta)\zeta_i + F_p(\Theta)\zeta_p \tag{6}$$

where $F_i(\Theta)$, $F_p(\Theta)$ are the dimensionless functions of protein coverage, and shape, and Θ is the dimensionless coverage of protein, calculated as

$$\Theta = S_g \left(\frac{Av}{M_w} \right) \Gamma_H \tag{7}$$

where S_g is the characteristic cross-section area of the albumin molecule (see Table 1).

As previously shown,[24,30] the functions $F_i(\Theta)$, $F_p(\Theta)$ can be approximated by the following analytical expressions:

Figure 5. Zeta potential of latex ζ versus the nominal coverage of rHSA, Γ_H [mg m^{-2}]. The points denote experimental results obtained for pH 3.5 and various NaCl concentrations: (a) 10^{-3} M, (b) 10^{-2} M, (c) 0.15 M. The solid lines show the results calculated from eqs 6−8 for the 3D electrokinetic model and the dashed dotted lines show the results calculated from the GC model, eqs 4−5.

$$F_i(\Theta) = e^{-C_i^0\theta}$$

$$F_p(\Theta) = \frac{1}{\sqrt{2}}\left(1 - e^{-\sqrt{2}C_p^0\theta}\right) \quad (8)$$

where, the C_i^0, C_p^0 constants depend on the κd_H parameter, where $\kappa^{-1} = (\varepsilon kT/2e^2I)^{1/2}$ is the double-layer thickness, $I = 1/2(\Sigma_i c_i z_i^2)$ is the ionic strength, and c_i the ion concentrations. For thin double layers, where $\kappa d_H > 1$, C_i^0, C_p^0 attain constant values of 10.2 and 6.5, respectively.[34] It should also be mentioned that for higher coverage the $F_i(\Theta)$ function vanishes and the $F_p(\Theta)$ function attains $1/\sqrt{2}$.

As can be seen in Figure 5c, the theoretical results calculated from eqs 6−8 reasonably agree with the experimental data for the ionic strength of 0.15 M. However, the effective cross-section area used in these calculations was 25 nm^2, significantly smaller than the geometrical cross-section area of albumin in the side-on orientation equal to 37 nm^2 (see Table 1). On the other hand, (Figure 5a,b) the 3D model overestimates the experimental data, predicting more abrupt increase of latex zeta potential with the albumin coverage. In this respect, our results deviate from previously obtained in the case of albumin (HSA) adsorption on mica where the 3D model was in a quantitative agreement with the experimental data for the entire range of ionic strength.[22] A most natural explanation of this difference is that in the case of albumin adsorption on latex particles there is a significant penetration of the molecule into the fuzzy polymeric layer. Therefore, only a limited part of the molecule surface, increasing with ionic strength, is exposed to the solution. This concept was previously used to explain fibrinogen adsorption on latex particles.[23] In contrast, because of the mica surface rigidity, the entire albumin surface area is exposed to the solution and the 3D model is valid for all ionic strengths.

From the data shown in Figure 5, one can estimate the maximum coverages of albumin defined as the points where the zeta potential of latex becomes constant. They are 1.0, 1.2, and 1.4 mg m^{-2} for NaCl concentration of 10^{-3}, 10^{-2}, and 0.15 M, respectively. These values, representing a first-order approximation of the maximum coverage of albumin, are given in Table 3.

It should be mentioned that the precision of this estimation is quite satisfactory for NaCl concentrations of 10^{-3} and 10^{-2} M. However, for the NaCl concentration of 0.15 M the maximum coverage estimation becomes less precise due to a small slope of the ζ versus Γ_H dependence (see Figure 5).

Because of the limited precision of the direct electrophoretic mobility measurements for higher salt concentration, two other methods were applied to determine the maximum coverage of albumin: the secondary electrokinetic method exploiting the

Table 3. Maximum Coverages of rHSA on Latex and HSA on Mica^a versus the Ionic Strength, pH 3.5

NaCl concentration [M]	$\kappa d_H/2$	electrophoretic mobility (EM)	depletion, centrifuge and EM	depletion (AFM)	HSA/mica streaming potential^a	theoretical (RSA modeling)
			maximum coverages [mg m^{-2}] obtained by various methods			
10^{-3}	0.42	1.0 ± 0.3	0.80 ± 0.2	0.70 ± 0.2	0.42	0.43
10^{-2}	1.15	1.2 ± 0.2	0.90 ± 0.2	1.0 ± 0.05	0.66	0.80
0.15	4.5	1.4 ± 03	1.1 ± 0.2	1.3 ± 0.1	1.3	1.3
∞	∞					1.74 (hard particles)

^{a}Previous data from ref 30.

calibrating measurements shown in Figure 5 and the above-described AFM method (see Figure 1).

Accordingly, in the former procedure, after the rHSA adsorption step, the latex suspension was centrifuged and a fixed volume of clear supernatant was acquired (see Figure 1). The supernatant containing an unknown concentration of albumin was mixed once again with pure latex suspension of the same bulk concentration as in the first step. The electrophoretic mobility (zeta potential) of the latex after the second adsorption step was again determined. The results of these experiments are shown in Figure 6 (for 10^{-2} NaCl) as the dependence of the zeta potential of latex on the initial albumin concentration added in the first step.
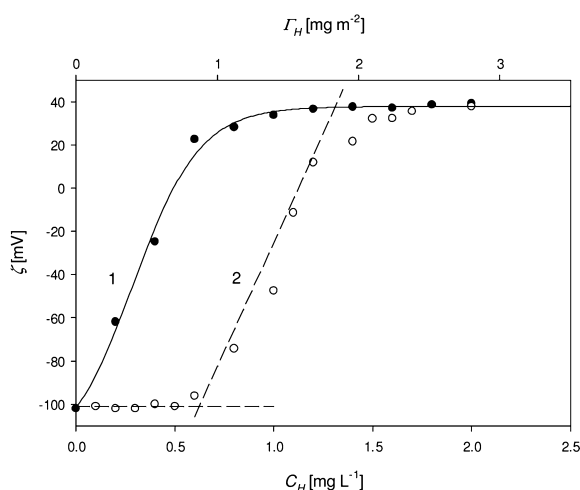
Figure 6. The dependencies of the zeta potential of latex ζ on the rHSA loading c_H expressed in mg L^{-1} (pH 3.5, 10^{-2} M, NaCl), lower axis. The upper axis shows the nominal coverage of rHSA Γ_H [mg m^{-2}] corresponding to this loading. Curve 1 denotes the reference line (smoothened) for the initial rHSA adsorption step and the dashed line 2 denotes the linear fits of the experimental data for the second adsorption step after suspension centrifugation (see Figure 1).

As can be observed, for low albumin concentration up to 0.7 mg L^{-1}, the change in latex zeta potential in the second step is negligible, which indicates that the final albumin concentration was zero. Only for c_H exceeding this threshold value, denoted by c_{Hv}, the latex zeta potential increases in an analogous manner as for the first adsorption step (shown by solid line in Figure 6). This threshold concentration can be accurately determined as the intersection point of this line with the horizontal line showing the zeta potential of bare latex (see Figure 6). Knowing c_{Hv}, one can calculate the maximum coverage of albumin on latex from eq 3. In this way, one obtains $\Gamma_{mx} = 0.9$ mg m^{-2} for the above case of 10^{-2} M NaCl and analogously 0.8 and 1.1 mg m^{-2} for 10^{-3}, and 0.15 M, NaCl, respectively. These data are collected in Table 3. As can be noticed, these electrokinetic data agree with previously discussed results obtained by direct microelectrophoretic method.

3.3. AFM Measurements. Because the centrifuging step is time-consuming, especially for low ionic strength, and may lead to suspension aggregation, an alternative AFM procedure was elaborated. It consists in determining the average number of albumin molecules per unit area of mica (surface concentration) N_{Hm} adsorbed after a fixed time via direct imaging. In these experiments, the original latex suspensions acquired after albumin adsorption were used. Because it was not filtered or

centrifuged, the reliability of this method is quite high. The single albumin molecules could be effectively imaged, because the deposition of latex particles on mica was negligible over the time of these experiments (1800 s) due to their minor number concentration and low diffusion coefficient compared to albumin molecules. Because the albumin adsorption is carried out under diffusion transport conditions, its surface concentration is governed by the formula[28]

$$N_{Hm} = 2\left(\frac{Dt}{\pi}\right)^{1/2} c_H \tag{9}$$

where t is the adsorption time.

Hence, for a fixed adsorption time (t_a), the albumin concentration in the suspension is proportional to the surface concentration of albumin on mica determined by AFM, that is, $c_H = CN_{Hm}$ where $C = \left[(\pi/4)Dt_a\right]^{1/2}$ is the constant.

The results of typical AFM measurements obtained for NaCl concentrations of 10^{-2} M are plotted in Figure 7 as the
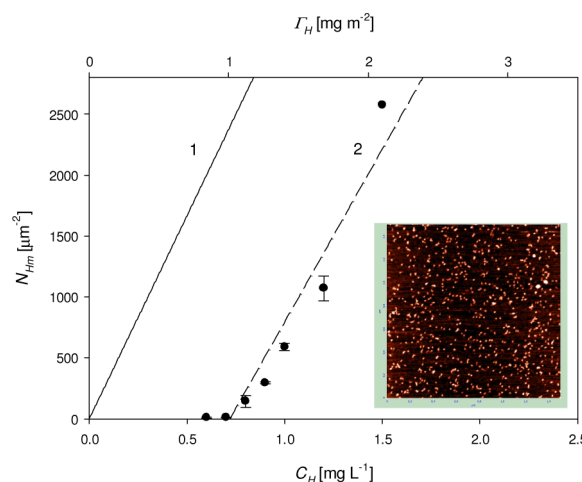
Figure 7. The dependencies of the surface concentration of rHSA on mica N_{Hm} determined by AFM imaging on the rHSA loading c_H expressed in mg L^{-1} (pH 3.5, 10^{-2} M, NaCl). The experimental procedure shown in Figure 1 was such that after the initial adsorption step, the latex suspension was contacted for 30 min with mica sheets in the diffusion cell. The solid line 1 shows the reference results predicted for diffusion-controlled transport of rHSA (calculated from eq 9), and the dashed line 2 shows the linear fits of experimental data. The inset shows rHSA monolayers on mica for the surface concentration of ca. 500 [μm^{-2}].

dependence of N_{Hm} on the initial concentration of albumin in the suspension. The inset to Figure 7 shows the AFM image of the typical albumin monolayer. Also, for comparison, the reference data, showing the dependence of N_{Hm} on albumin concentration in pure solutions without contacting the latex (attained after 1800 s) are shown in Figure 7 (solid line number 1).

As can be observed, for low c_H the surface concentration N_{Hm} was negligible indicating, according to eq 9, that there was no residual albumin in the suspension. Measurable values of N_{Hm} only appeared for the initial albumin concentrations exceeding the threshold value c_{Ht}. This value can be precisely determined as the intersection of the straight line approximating the experimental data with the x-axis (see Figure 7). Knowing c_{Hv}, one can calculate the maximum albumin coverage from eq 3, analogously as in the previous case.

In this way, one obtains Γ_{mx} = 0.7, 1.0, and 1.3 mg m^{-2} for NaCl concentrations of 10^{-3}, 10^{-2}, and 0.15 M, respectively (see Table 3). It should be mentioned that the AFM procedure is more reliable than the two previous methods, assuring a relative precision of measurements of about 0.05 mg m^{-2}. As can be deduced, the maximum coverage of albumin on latex increases with ionic strength, that is, the κd_H parameter suggesting that this effect is caused by the lateral electrostatic interactions among adsorbed molecules. This hypothesis is further supported by the fact that analogous results were reported in the literature for colloid particles,[35] dendrimers,[36] gold,[34] silver nanoparticles,[37] human serum albumin,[22] and fibrinogen on latex.[23] This effect was accounted for by using the effective hard particle concept.[24,38] The following expression for the maximum coverage of the protein can be formulated

$$\Gamma_{mx} = \Gamma_{\infty} \frac{1}{\left(1 + \frac{2h^*}{d_H}\right)^2} \tag{10}$$

where Γ_{∞} is the maximum coverage for hard (noninteracting) molecules and $2h^*$ is the characteristic distance between particle surfaces where the repulsive electrostatic interaction energy tends to infinity.[38]

This parameter, characterizing the repulsive double-layer interactions particles, can be calculated from the formula[38]

$$\frac{2h^*}{d_H} = \frac{1}{\kappa d_H}\left\{\ln\frac{\phi_0}{2\phi_{ch}} - \ln\left[1 + \frac{1}{\kappa d_H}\ln\frac{\phi_0}{2\phi_{ch}}\right]\right\} \tag{11}$$

where ϕ_0 is the characteristic interaction energy of two albumin molecules and ϕ_{ch} is the scaling interaction energy, close to the kT unit.

The maximum coverage for hard particles Γ_{∞} can be calculated from the formula

$$\Gamma_{\infty} = \left(\frac{M_w}{S_g Av}\right)\Theta_{\infty} \tag{12}$$

where Θ_{∞} is the dimensionless maximum coverage that can be derived from random sequential adsorption (RSA) simulations.[39−41] For hard particles of a spherical shape, Θ_{∞} = 0.547. This value is slightly dependent on the shape of the particle (molecule), for example, for a spheroidal particles of the long to short axis ratio equal to 2, Θ_{∞} = 0.583.[41] Taking the latter value one obtains from eq 12 that Γ_{∞} = 1.74 mg m^{-2}. Therefore, from eqs 10 and 11 one can calculate that the theoretical maximum coverage for 0.15 M NaCl should be 1.3 mg m^{-2}, which matches the experimental value. It is also the same as previously determined from the HSA adsorption on mica where the coverage was determined via in situ streaming potential measurements.[22] On the other hand, for 10^{-3} M NaCl the theoretically predicted coverage is 0.43 mg m^{-2} that is considerably less than our experimental value of 0.7 mg m^{-2} (see Table 3). In the case of the HSA/mica system, the experimental coverage was 0.42 mg m^{-2}. A most probable explanation of this difference should be sought in the albumin penetration into the fuzzy polymeric layer on latex particles, above suggested by the electrophoretic mobility measurements (see Figure 5). Hence, the lateral interactions among adsorbed albumin molecules are more effectively screened due to the presence of negatively charged polymer chains than for bare mica.

It is interesting to mention that our results agree with previously obtained for other albumins. For example, Norde and Lyklema[9] determined that the coverage of irreversibly bound HSA at negatively charged polystyrene latexes was ca. 1 mg m^{-2} for pH 4 and ionic strength of 5 × 10^{-2} M.

A similar study of BSA adsorption at carboxylated PS/PMAA microspheres was done by Yoon et al.[42] who obtained 0.8−1.0 mg m^{-2} as the maximum coverage of BSA for pH 3.3 and ionic strength of 10^{-2} M in the limit of low bulk concentration.

4. CONCLUSIONS

Microelectrophoretic and AFM measurements furnished reliable clues on the mechanisms of recombinant albumin adsorption on polystyrene latex particles at pH 3.5 and NaCl concentrations varying between 10^{-3} and 0.15 M.

It was shown that albumin adsorption was irreversible and the monolayers formed on latex are stable in time. The maximum coverage determined by the improved depletion method varied between 0.7 mg m^{-2} for 10^{-3} M NaCl to 1.3 mg m^{-2} for 0.15 M NaCl. The latter value matches the maximum coverage previously determined for human serum albumin on mica using the streaming potential method. The increase in the maximum coverage was interpreted in terms of reduced electrostatic repulsion among adsorbed protein molecules. Therefore, it was concluded that albumin adsorption at pH 3.5 is governed by electrostatic interactions and proceeds analogously to colloid particle deposition.

Two practical aspects of the work were envisaged: (i) developing a method of determining albumin bulk concentration at the level of 0.1 mg L^{-1} (ca. 10^{-9} M) via the simple microelectrophoretic measurements and (ii) developing a robust procedure of preparing stable albumin monolayers on latex particles of well-controlled coverage and molecule distribution.

■ ASSOCIATED CONTENT

ⓢ Supporting Information
Additional figure. This material is available free of charge via the Internet at http://pubs.acs.org.

■ AUTHOR INFORMATION

Corresponding Author
*E-mail: ncadamcz@cyf-kr.edu.pl.
Notes
The authors declare no competing financial interest.

■ ACKNOWLEDGMENTS

■ REFERENCES

(1) Carter, D. C.; Ho, J. X. Structure of serum albumin. *Adv. Protein Chem.* **1994**, *45*, 153−203.

(2) Peters, T., Jr. Serum Albumin. *Adv. Protein Chem.* **1985**, *37*, 161−245.

(3) Martín-Rodríguez, A.; Ortega-Vinuesa, J. L.; Hidalgo-Álvarez, R. Electrokinetics of protein-coated latex particles. In *Interfacial Electrokinetics and Electrophoresis*; Delgado, Á. V., Ed.; Surfactant Science; Marcel Dekker, Inc.: New York, 2002; pp 641−670.

(4) Norde, W. Adsorption of proteins from solution at the solid-liquid interface. *Adv. Colloid Interface Sci.* **1986**, *25*, 267−340.

(5) Haynes, C. A.; Norde, W. Globular proteins at solid/liquid interfaces. *Colloids Surf., B* **1994**, *2*, 517−566.

(6) RCSB Protein Data Bank http://www.pdb.org/, accessed Dec 28, 2011.

(7) Rezwan, K.; Meier, L. P.; Gauckler, L. J. A prediction method for the isoelectric point of binary protein mixtures of bovine serum albumin and lysozyme adsorbed on colloidal titania and alumina particles. *Langmuir* **2005**, *21*, 3493−3497.

(8) Jachimska, B.; Wasilewska, M.; Adamczyk, Z. Characterization of globular protein solutions by dynamic light scattering, electrophoretic mobility, and viscosity measurements. *Langmuir* **2008**, *24*, 6866−6872.

(9) Norde, W.; Lyklema, J. The adsorption of human plasma albumin and bovine pancreas ribonuclease at negatively charged polystyrene surfaces: I. Adsorption isotherms. Effects of charge, ionic strength, and temperature. *J. Colloid Interface Sci.* **1978**, *66*, 257−265.

(10) Koutsoukos, P. G.; Mummé-Young, C. A.; Norde, W.; Lyklema, J. Effect of the nature of the substrate on the adsorption of human plasma albumin. *Colloids Surf.* **1982**, *5*, 93−104.

(11) Radomska-Galant, I.; Basińska, T. Poly(styrene/α-tert-butoxy-ω-vinylbenzylpolyglycidol) Microspheres for Immunodiagnostics. Principle of a Novel Latex Test Based on Combined Electrophoretic Mobility and Particle Aggregation Measurements. *Biomacromolecules* **2003**, *4*, 1848−1855.

(12) Słomkowski, S.; Kowalczyk, D.; Chehimi, M. M.; Dealamar, M. X-ray photoelectron spectroscopy as a tool for studies of the surface layer of microspheres. The case of polystyrene and poly(styrene−acrolein) microspheres with attached human serum albumin. *Colloid Polym. Sci.* **2000**, *278*, 878−883.

(13) Rezwan, K.; Meier, L. P.; Rezwan, M.; Vörös, J.; Textor, M.; Gauckler, L. J. Bovine serum albumin adsorption onto colloidal Al₂O₃ particles: a new model based on zeta potential and UV−Vis measurements. *Langmuir* **2004**, *20*, 10055−10061.

(14) Oliva, F. Y.; Avalle, L. B.; Cámara, O. R.; De Pauli, C. P. Adsorption of human serum albumin (HSA) onto colloidal TiO₂ particles, Part I. *J. Colloid Interface Sci.* **2003**, *261*, 299−311.

(15) Kaufman, E. D.; Belyea, J.; Johnson, M. C.; Nicholson, Z. M.; Ricks, J. L.; Shah, P. K.; Bayless, M.; Pettersson, T.; Feldotö, Z.; Blomberg, E.; Claesson, P.; Franzen, S. Probing protein adsorption onto mercaptoundecanoic acid stabilized gold nanoparticles and surfaces by quartz crystal microbalance and ζ-potential measurements. *Langmuir* **2007**, *23*, 6053−6062.

(16) Van Dulm, P.; Norde, W. The adsorption of human plasma albumin on solid surfaces, with special attention to the kinetic aspects. *J. Colloid Interface Sci.* **1983**, *91*, 248−255.

(17) Elgersma, A. V.; Zsom, R. L. J.; Lyklema, J.; Norde, W. Kinetics of single and competitive protein adsorption studied by reflectometry and streaming potential measurements. *Colloids Surf.* **1992**, *65*, 17−28.

(18) Malmsten, M. Ellipsometry studies of protein layers adsorbed at hydrophobic surfaces. *J. Colloid Interface Sci.* **1994**, *166*, 333−342.

(19) Kurrat, R.; Ramsden, J. J.; Prenosil, J. E. Kinetic model for serum albumin adsorption: experimental verification. *J. Chem. Soc., Faraday Trans.* **1994**, *90*, 587−590.

(20) Kurrat, R.; Prenosil, J. E.; Ramsden, J. J. Kinetics of human and bovine serum albumin adsorption at silica−titania surfaces. *J. Colloid Interface Sci.* **1997**, *185*, 1−8.

(21) Ortega-Vinuesa, J. L.; Tengvall, P.; Lundström, I. Molecular packing of HSA, IgG, and fibrinogen adsorbed on silicon by AFM imaging. *Thin Solid Films* **1998**, *324*, 257−273.

(22) Dąbkowska, M.; Adamczyk, Z. Ionic strength effect in HSA adsorption on mica determined by streaming potential measurements. *J. Colloid Interface Sci.* **2012**, *366*, 105−113.

(23) Bratek-Skicki, A.; Żeliszewska, P.; Adamczyk, Z.; Cieśla, M. Human Fibrinogen Monolayers on Latex Particles: Role of Ionic Strength. *Langmuir* **2013**, *29*, 3700−3710.

(24) Adamczyk, Z.; Sadlej, K.; Wajnryb, E.; Nattich, M.; Ekiel-Jeżewska, M. L.; Bławzdziewicz, J. Streaming potential studies of colloid, polyelectrolyte and protein deposition. *Adv. Colloid Interface Sci.* **2010**, *153*, 1−29.

(25) He, X. M.; Carter, D. C. Atomic structure and chemistry of human serum albumin. *Nature* **1992**, *358*, 209−215.

(26) Laemmli, U. K. Cleavage of structural proteins during the assembly of the head of bacteriophage T4. *Nature* **1970**, *227*, 680−685.

(27) Goodwin, J. W.; Hearn, J.; Ho, C. C.; Ottewill, R. H. Studies on the preparation and characterisation of monodisperse polystyrene laticee. III. Preparation without added surface active agents. *Colloid Polym. Sci.* **1974**, *252*, 464−471.

(28) Adamczyk, Z.; Bratek-Skicki, A.; Dąbrowska, P.; Nattich-Rak, M. Mechanisms of fibrinogen adsorption on latex particles determined by zeta potential and AFM measurements. *Langmuir* **2012**, *28*, 474−485.

(29) Wasilewska, M.; Adamczyk, Z.; Jachimska, B. Structure of Fibrinogen in electrolyte solutions derived from dynamic light scattering (DLS) and viscosity measurements. *Langmuir* **2009**, *25*, 3698−3704.

(30) Wasilewska, M.; Adamczyk, Z. Fibrinogen adsorption on mica studied by AFM and in situ streaming potential measurements. *Langmuir* **2011**, *27*, 686−696.

(31) Serra, J.; Puig, J. E.; Martín, Á.; Galisteo, F. C.; Gálvez, M. J.; Hidalgo-Álvarez, R. On the adsorption of IgG onto polystyrene particles: electrophoretic mobility and critical coagulation concentration. *Colloid Polym. Sci.* **1992**, *270*, 574−583.

(32) Adamczyk, Z.; Nattich, M.; Wasilewska, M.; Zaucha, M. Colloid particle and protein deposition - Electrokinetic studies. *Adv. Colloid Interface Sci.* **2011**, *168*, 3−28.

(33) Sadlej, K.; Wajnryb, E.; Bławzdziewicz, J.; Ekiel-Jeżewska, M. L.; Adamczyk, Z. Streaming current and streaming potential for particle covered surfaces: Virial expansion and simulations. *J. Chem. Phys.* **2009**, *130*, No. 144706.

(34) Brouwer, E. A. M.; Kooij, E. S.; Wormeester, H.; Poelsema, B. Ionic strength dependent kinetics of nanocolloidal gold deposition. *Langmuir* **2003**, *19*, 8102−8108.

(35) Zaucha, M.; Adamczyk, Z.; Barbasz, J. Zeta potential of particle bilayers on mica: A streaming potential study. *J. Colloid Interface Sci.* **2011**, *360*, 195−203.

(36) Pericet-Camara, R.; Cahill, B. P.; Papastavrou, G.; Borkovec, M. Nano-patterning of solid substrates by adsorbed dendrimers. *Chem. Commun.* **2006**, 266−268.

(37) Oćwieja, M.; Adamczyk, Z.; Morga, M.; Michna, A. High density silver nanoparticle monolayers produced by colloid self-assembly on polyelectrolyte supporting layers. *J. Colloid Interface Sci.* **2011**, *364*, 39−48.

(38) Adamczyk, Z. Particles at Interfaces: Interactions, Deposition, Structure. *Interface Science and Technology*, 1st ed.; Academic Press: Amsterdam, 2006.

(39) Hinrichsen, E. L.; Feder, J.; Jøssang, T. Geometry of random sequential adsorption. *J. Stat. Phys.* **1986**, *44*, 793−827.

(40) Schaaf, P.; Talbot, J. Surface exclusion effects in adsorption processes. *J. Chem. Phys.* **1989**, *91*, 4401−4409.

(41) Viot, P.; Tarjus, G.; Ricci, S. M.; Talbot, J. Random sequential adsorption of anisotropic particles. I. Jamming limit and asymptotic behavior. *J. Chem. Phys.* **1992**, *97*, 5212−5218.

(42) Yoon, J.-Y.; Park, H.-Y.; Kim, J.-H.; Kim, W.-S. Adsorption of BSA on Highly Carboxylated Microspheres—Quantitative Effects of Surface Functional Groups and Interaction Forces. *J. Colloid Interface Sci.* **1996**, *177*, 613−620.